



Numerical Assessment of the Deformation of CFRD Dams During Earthquakes

A. O. Sfriso
LMNI, Faculty of Engineering, University of Buenos Aires, Argentina

Keywords: CFRD dams, earthquakes, plasticity, seismic analysis.

ABSTRACT: A numerical procedure for the preliminary estimation of the earthquake-induced settlement of concrete face rockfill dams is presented. The method is based on a simple constitutive model that accounts for the key features of the behavior of coarse grained materials that affect the response of CFRDs, namely pressure dependent elasticity and a peak friction angle dependent on both pressure and void ratio. The actual earthquake design record is replaced by a simple sinusoidal base acceleration having an equivalent effect on the dam. The numerical model uses isotropic hyperelasticity and isotropic hardening/softening plasticity combined with stress-dilatancy theory, and thus is applicable to geometries and materials where only monotonic plasticity is expected to occur, as is the case of CFRD dams. A case study is presented where the procedure is applied to a CFRD 140 m high, located in Argentina and designed for a strong earthquake. The computed settlement compares well with an analytical estimation and with a decoupled numerical model of the same problem. The main advantage of the proposed procedure is that all material nonlinearities are accounted for by the constitutive equations, thus allowing for the usage of a simple mesh with no artificial sub-zonification.

1 Introduction

Concrete Face Rockfill Dam (CFRD) engineering has reached a mature state in many aspects, including foundation design, selection procedures for construction materials, zonification criteria, compaction methods and construction procedures for the concrete face. Design of CFRDs is, however, still based on experience and engineering judgement (Cooke, 1984; Cooke, 1997; Núñez, 2007b). When placed in areas of high seismicity, an assessment of the effects of strong earthquakes on the overall behavior of CFRDs is required. Performance rather than safety is the main concern, as it is widely accepted that the effect of seismic loading on CFRDs is plastic deformation and settlement but not a slope failure in its classical sense (Cooke, 1984; Gazetas and Dakoulas, 1992; Makdisi and Seed, 1978; Newmark, 1965; Seed, 1979).

Freeboard allowance for earthquake-induced settlements may exceed 1% of the dam's height. In the current state of the art, this allowance cannot be significantly reduced by design efforts and is weakly dependent on the dam's geometry and materials (Núñez, 2007b). Therefore, the problem can be posed as follows: verify that the minimum freeboard is enough for your dam; if not, increase the freeboard or modify your design otherwise.

The design of the concrete face for earthquake loading poses additional challenges. While the concrete face is just a water barrier and not a structural member of the dam, its structural behavior must be verified at design stage. To date, design efforts are limited to avoid in-plane compressive failure, to minimize cracking and to assure a dependable behavior of the concrete joints. Provisions are taken to avoid pore pressures to develop in the dam's body during and after strong seismic shaking (Cooke and Sherard, 1987; Sherard and Cooke, 1987).

Methods used to estimate earthquake-induced dam deformation range from simple analytical tools (Newmark, 1965; Makdisi and Seed, 1978; Núñez, 2007) to involved three dimensional (3D) numerical models. While analytical tools are simple to use, they cannot take into account special features of dam design, like zonification, existence of berms or non uniform slopes. On the other hand, the reliability of numerical methods heavily depends on the choice of the constitutive models and the selection of input parameters. Moreover, 3D numerical models are too involved to be used at design stage.

The goal is to advance in the development of simple methods to estimate earthquake-induced deformation of dams at design stage. Due to dam zonification, numerical methods appear to be the natural choice. Due to the uncertainties in material properties, simple constitutive models should be adopted. Finally, uncertainties in earthquake loading favors the adoption of conservative, synthetic seismic records. Design is always followed by

analysis, where 3D nonlinear models can be performed to account for construction processes, relevant features of construction materials and selected seismic records. For simplicity, in this paper only CFRDs resting on hard rock are considered. The suggested procedure, however, can accommodate any foundation type.

2 Earthquake-induced deformation of dams

2.1 Sliding block conceptual model

The conceptual problem can be best understood with the aid of the sliding block model (Newmark, 1965). A rigid block rests on a plane having a block-surface friction angle ϕ and an inclination $\beta < \phi$, see Fig. 1a. The block can resist a maximum static force T_s parallel to the slope of magnitude

$$T_s = (\sin[\phi - \beta] / \cos[\phi]) mg \quad (1)$$

where m is the mass of the block and g is the acceleration of gravity. Inertia forces appear when the system is accelerated to the right with an acceleration $a = \lambda g$, see Fig. 1b. During the application of this acceleration, T_s is reduced to a dynamic value T_d of magnitude

$$T_d = (\sin[\phi - \beta] / \cos[\phi] - \lambda \cos[\phi - \beta] / \cos[\phi]) mg \quad (2)$$

which can be negative if $\lambda > \lambda_c$, where

$$\lambda_c = \tan[\phi - \beta] \quad (3)$$

is a threshold acceleration coefficient. An acceleration λg large enough to produce a negative T_d acting during a period Δt produces a net downwards displacement δ of the block on the base surface which is the sum of the displacement at the acceleration phase, and the displacement of the braking phase

$$\delta = \frac{1}{2} \frac{\|T_d\|}{m} \Delta t^2 + \frac{1}{2} \frac{\|T_s\|}{m} \Delta t_b^2 \quad (4)$$

where $\Delta t_b = \|T_d / T_s\| \Delta t$ is the duration of the braking phase. After some algebra, the final expression is

$$\delta = \lambda g \frac{\cos[\phi - \beta]}{2 \cos[\phi]} \left(\frac{\lambda}{\tan[\phi - \beta]} - 1 \right) \Delta t^2 \quad (5)$$

A series of random pulses acting on the system produces a cumulative displacement that is the sum of the contribution of the individual pulses of the series. All pulses having $\lambda < \lambda_c$ produce no effect. It is a common assumption that negative pulses, acting leftwards in Fig. 1b, are not large enough to produce upwards displacements of the block (Newmark, 1965; Makdisi and Seed, 1978). This implies that cyclic earthquake loading, however complex it may be, only produces monotonic plastic deformations to the system.

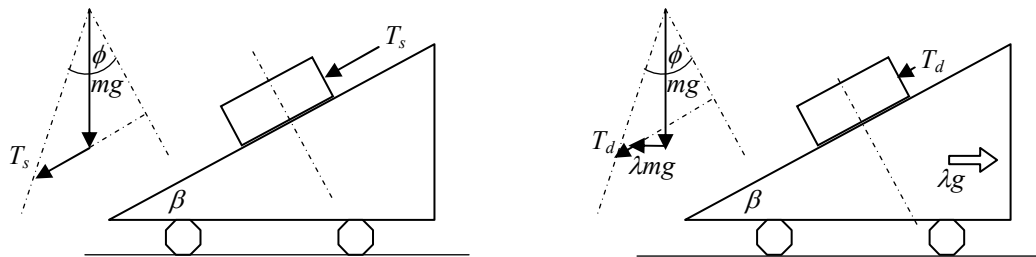


Fig. 1. Sliding block model. a) static stability. b) stability of the accelerated system.

2.2 Extension to dam's geometry

A dam can be understood as a triangular body of earth-like material where sliding wedges can form with any shape and size, provided limit state conditions are reached in the sliding surface. Moreover, an earthquake can be understood as a large series of positive and negative acceleration pulses acting on the base of the dam and propagating through the dam's body (Makdisi and Seed, 1978; Gazetas and Dakoulas, 1992). A given wedge

has a particular λ_c which depends on the inclination of the potential sliding surface of the wedge. Pulses having $\lambda < \lambda_c$ produce no net displacement between the wedge and the rest of the dam's body and are termed non effective pulses. Effective positive pulses produce no effect on the potential wedges at one side of the dam, while effective negative pulses produce no effect on the other side. Total settlement of the dam is the contribution of the vertical component of the downwards displacement of all wedges in both sides of the dam. For CFRDs, a full reservoir implies that water pressure stabilizes the potential wedges on the upstream slope. Therefore, for a given CFRD and earthquake, total settlement of the dam with empty reservoir is larger than the settlement of the dam with full reservoir (Uddin and Gazetas, 1995; Núñez, 2007).

2.3 Equivalent earthquake

The dam is a dynamic system that propagates stress waves through the dam body, producing wave amplification, attenuation and interference that result in a complex 3D response. The overall response of the dam depends on its natural period compared with the dominant period of the earthquake. The natural period of the dam, in turn, depends on the geometry of the dam, the elastic properties of the construction materials and the interaction between the dam and its foundation. For triangular, uniform, elastic dams of infinite length, the natural period T can be computed with (Gazetas and Dakoulas, 1992)

$$T = 2.61H/v_s \quad (6)$$

where H is the height of the dam

$$v_s = \sqrt{G/\rho} \quad (7)$$

is the shear wave velocity of the dam material, G is the shear modulus and ρ is the material density. For other dam shapes, Núñez (Núñez, 2007) proposed a procedure to compute T that can be condensed into

$$T = 2.61 \frac{H}{v_s} \frac{12\alpha_c^2 + 16(\alpha_b + \alpha_c)}{32 + 36\alpha_c + 9\alpha_c^2} \quad (8)$$

where $\alpha_c = l_c/H$, $\alpha_b = l_b/H$, l_c is the crest and l_b is the base length of the dam.

An earthquake can be defined by its magnitude M and its peak ground acceleration PGA . A simple correlation between M and the effective number of pulses N is (Núñez, 2007)

$$N = M - 1 \quad (9)$$

Therefore, the simplest dynamic loading that approximates the effect of a real earthquake loading is a sinusoidal wave action of amplitude PGA , period T and duration $t = NT$. This acceleration record is too conservative, as PGA only occurs once in a given earthquake, Núñez (Núñez, 2007) proposed to use a max. acceleration $a_{max} = \eta PGA$ with η depending on the earthquake type in the range $0.8 < \eta < 0.9$.

3 Material properties relevant for the analysis

3.1 Elasticity

Dams are built by compaction of layers of rockfill, a fact that impairs orthotropic properties to the material. The limited information on material properties available at design stage, however, deems the application of orthotropic elasticity impractical, and therefore isotropic elasticity is usually assumed. The shear modulus of the rockfill is often computed with the expression (Hardin and Richart, 1963; Kokusho, 1980)

$$G = c_s \frac{(c_e - e)^2}{1 + e} \left(\frac{p}{p_{ref}} \right)^m p_{ref} \quad (10)$$

where c_s , c_e and m are material parameters, e is void ratio, p is mean pressure and p_{ref} is a reference pressure usually adopted equal to atmospheric pressure. Elastic bulk modulus has a minor influence in most problems involving CFRDs. It can be computed with the shear modulus and an assumed Poisson's ratio in the range $0.15 < \nu < 0.30$ for dense gravels and rockfills.

3.2 Peak friction angle

It is widely recognized that the peak friction angle of granular materials depends on mean pressure and void ratio (De Beer, 1965; Marsal, 1967). Bolton (1986) introduced the expression

$$\phi_{ic} = \phi_c + 3^\circ D_r (Q - \ln[p/1 \text{ KPa}]) - 3^\circ \quad (11)$$

where ϕ_{ic} is the peak friction angle for triaxial compression, ϕ_c is the critical state (CS) friction angle, D_r is relative density and Q is a material parameter accounting for particle strength.

The dependence of ϕ_{ic} on void ratio is rarely acknowledged for in dam design, as material parameters are determined for the specified compaction void ratio. An expression frequently used to estimate the peak friction angle of rockfills is (Duncan et al, 1980; Leps, 1970)

$$\phi_{ic} = \phi_0 - \Delta\phi \log[p/p_{ref}] \quad (12)$$

where ϕ_0 and $\Delta\phi$ are material parameters.

While Eqn. 12 properly accounts for the reduction of ϕ_{ic} with increasing pressure, it fails to capture its evolution with plastic strain, and therefore demands for the adoption of a set of parameters ϕ_0 and $\Delta\phi$ consistent with the assumed level of material softening for a given seismic action. Sfriso (2007) introduced the expression

$$\phi_{ic} = \phi_c - A D_r \log[\chi] - B \quad (13)$$

where $A = 3^\circ$, $B = 1^\circ$ and

$$\chi = (p e^{2.5}) / (p_r p_{ref}) \quad (14)$$

is a measure of stress level and p_r is a material parameter accounting for particle strength. Eqn. (13) is conceptually equivalent to Eqn. (11) except for the fact that χ is void-ratio dependent while the equivalent term $p/\exp[Q]$ is not. Dependency of χ on void ratio reflects the higher crushing resistance of particles for increasing number of contacts per particle, i.e. at denser states.

As pointed out by Bolton (1986), a minimum pressure $p = 150 \text{ KPa}$ should be used in Eqn. (11) and subsequently in Eqn. (14) to avoid the use of an unsafe friction angle due to overestimation of dilatancy. Eqn. (13) yields $\phi_{ic} = \phi_c$ (i.e. CS behavior) at a pressure

$$p = p_r e^{-2.5} \exp[-B/(A D_r)] p_{ref} \quad (15)$$

Fig. 2a shows ϕ_{ic} of Toyoura sand (Bolton, 1987) for different pressures and void ratios and the prediction by Eqn. (13) with $p_r = 40$ and $\phi_c = 32.5^\circ$. Fig. 2b shows the CS void ratio e_c for Toyoura sand (Verdugo and Ishihara, 1996) and the prediction by Eqn. (15) with the same set of material parameters. The good agreement shown implies that Eqn. (13) has the capability to reproduce that $e \rightarrow e_c$ implies $\phi_{ic} \rightarrow \phi_c$.

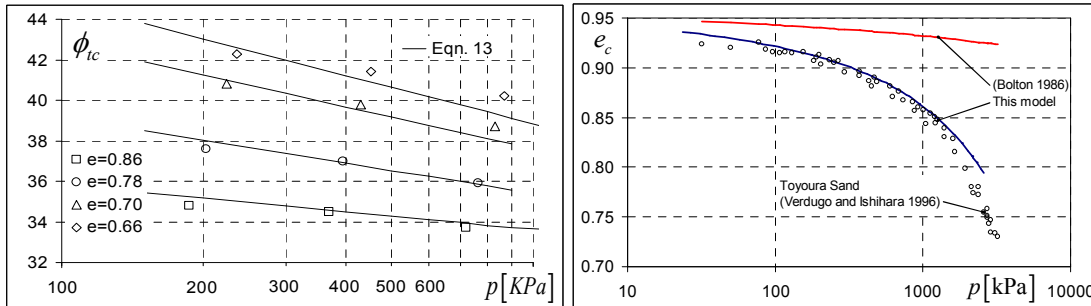


Fig. 2. a: Peak friction angle as a function of mean pressure and void ratio, Toyoura sand. Predicted vs. experimental results. b: critical state line for Toyoura sand. Predicted vs. experimental results.

A CFRD subjected to an earthquake is a plane strain problem even for irregular valley shapes, and therefore a plane strain peak friction angle ϕ_{ps} should be adopted. It is usual to use the estimation $\phi_{ps} = 1.15 \phi_{ic}$.

3.3 Stress-strain

A vast literature exists on the application of moduli reduction curves and damping coefficients to the decoupled analysis of earthquake loading to dams (e.g. Duncan et al, 1980; Kokusho, 1980; Seed et al, 1984). For a coupled analysis, however, simple failure plasticity can account for much of the energy dissipation normally attributed to damping and nonlinear stress-strain response.

A simple exercise can prove this assessment. A symmetric triangular dam 100m high with slopes 1.4:1 was subjected to a wave acceleration of $PGA = 0.5$ for a duration $t = 6T = 2.4s$ and left free to oscillate for another $t = 2.4s$. The hyperbolic model available in Plaxis (Duncan and Chang, 1970; Brinkgreve, 2002) was

used with the following parameters: $\gamma = 23.5 \text{ KN/m}^3$, $E_{ur}^{ref} = 370 \text{ MN/m}^3$, $m = 0.5$, $\nu = 0.2$, $c = 1 \text{ KN/m}^3$, $\phi = 50^\circ$. Parameters controlling the stress-strain response of the model were varied as shown in Table 1. For the meaning of the parameters of the hyperbolic model refer to (Brinkgreve, 2002). Triangular 15 noded elements with an average size of 5 m were used along with an absorbent base boundary. δ is the vertical settlement of the crest of the dam at the end of the simulation.

Table 1. Material parameters for the sensitivity analysis of the hyperbolic model.

E_{50}^{ref}	MN/m^2	80	120	160	80	120	160	80	120	160
R_f	-	0.50	0.50	0.50	0.75	0.75	0.75	1.00	1.00	1.00
δ	m	2.03	1.95	1.93	1.98	1.92	1.95	1.94	1.97	1.98

It is worth noting that all results fall within $\delta = 1.98 \text{ m} \pm 2.5\%$, despite the fact that the parameters controlling the stress-strain response, namely E_{50}^{ref} and R_f where varied beyond their usual bounds.

4 A simple constitutive model for coarse grained granular materials

4.1 Formulation

A simple elastoplastic model for the preliminar assessment of earthquake-induced deformation of dams is presented. The model uses pressure dependent hyperelasticity and non-associative isotropic hardening-softening plasticity in the post-failure regime. Hardening is due solely to the evolution of ϕ_{tc} with void ratio. Material parameters are the already mentioned c_s , c_e , m , ϕ_c , p_r along with e_{min} and e_{max} , the min. and max. void ratios used to compute D_r . The state of the material is characterized by the Cauchy stress $\boldsymbol{\sigma}$ and the void ratio e . Standard additive decomposition of the infinitesimal strain tensor rate $\dot{\boldsymbol{\epsilon}}$ is adopted. It holds

$$\dot{\boldsymbol{\epsilon}} = \dot{\boldsymbol{\epsilon}}^e + \dot{\boldsymbol{\epsilon}}^p \quad (16)$$

where $\dot{\boldsymbol{\epsilon}}^e$ and $\dot{\boldsymbol{\epsilon}}^p$ are the elastic and plastic strain tensor rates. Stress-strain equation is of the form

$$\boldsymbol{\sigma} = \partial W_s / \partial \boldsymbol{\epsilon}^e \quad (17)$$

where W_s is a complementary strain energy function of state variables $\{\boldsymbol{\sigma}, e\}$ of the form (Molenkamp, 1988)

$$W_s = \frac{p^2}{G} \left(\frac{2 - D_r}{3(1-m)(2-m)} + \frac{r^2}{4} \right) \quad (18)$$

where $r = \|\mathbf{r}\|$, $\mathbf{r} = \mathbf{s} / p$, $\mathbf{s} = \boldsymbol{\sigma} - p\mathbf{1}$ and $\mathbf{1}$ is the second order unit tensor. G is computed with Eqn. (10). Bulk modulus, as derived from Eqn. (18), is

$$K = \frac{G}{\frac{2-D_r}{3(1-m)} - \frac{m}{4} r^2} \quad (19)$$

yielding a Poisson's ratio $0.05 < \nu < 0.23$ for $0 < D_r < 1$.

The yield function is a modified version of the Matsuoka-Nakai yield function of the form (Matsuoka and Nakai, 1974)

$$F = \frac{1}{2}(\mu + 6)\mathbf{r} : \mathbf{r} - \frac{1}{3}(\mu + 9)\mathbf{r} \cdot \mathbf{r} : \mathbf{r} - \mu = 0 \quad (20)$$

where (\cdot) and $(:)$ denote simple and double contraction and

$$\mu = 8 \tan^2 [\phi_{tc}] \quad (21)$$

ϕ_{tc} is computed with Eqn. (13). The effect of the intermediate principal stress on shear strength (i.e. the difference between ϕ_{tc} and ϕ_{ps}) is properly accounted for by Eqn. (20). The plastic shear rate is of the form

$$\dot{\boldsymbol{\epsilon}}^p = \dot{\lambda} \mathbf{m} \quad (22)$$

where $\dot{\lambda}$ is a plastic multiplier and \mathbf{m} is the plastic strain rate unit tensor of the form

$$\mathbf{m} = \mathbf{m}_d + \beta \mathbf{1} \quad (23)$$

The deviatoric component of the flow direction in shear \mathbf{m}_d is given by

$$\mathbf{m}_d = \mathbf{n}_d / \|\mathbf{n}_d\| \quad (24)$$

where $\mathbf{n}_d = \mathbf{n} - \frac{1}{3}(\mathbf{n} : \mathbf{1})\mathbf{1}$ and $\mathbf{n} = F_{\sigma}$ is the (outwards) normal to the yield function.
 β is computed after stress-dilatancy theory (Rowe, 1962) as (Sfriso, 2007)

$$\beta = \begin{cases} -(\sigma_1 m_{d1} + \sigma_2 m_{d2} + N_c \sigma_3 m_{d3}) / (\sigma_1 + \sigma_2 + N_c \sigma_3) \leftarrow m_{d2} + \beta > 0 \\ -(\sigma_1 m_{d1} + N_c (\sigma_2 m_{d2} + \sigma_3 m_{d3})) / (\sigma_1 + N_c (\sigma_2 + \sigma_3)) \leftarrow m_{d2} + \beta < 0 \end{cases} \quad (25)$$

where $\{\sigma_1, \sigma_2, \sigma_3\}$ and $\{m_{d1}, m_{d2}, m_{d3}\}$ are the sorted eigenvalues of $\boldsymbol{\sigma}$ and \mathbf{m}_d and

$$N_c = (1 + \sin[\phi_c]) / (1 - \sin[\phi_c]) \quad (26)$$

Evolution of the state variable e is of the form

$$\dot{e} = (1 + e) \dot{\varepsilon}_v^p \quad (27)$$

The concept underlying this formulation is that the initial state is denser/looser than the critical state, and hence $\phi_{ic} \neq \phi_c$. Plastic shearing produces a change in void ratio which is obtained by time integration of Eqn. (27), where $\dot{\varepsilon}_v^p = 3\beta\lambda$. This change in void ratio affects ϕ_c and the aperture of the failure cone given by Eqn. (20). Continued shearing attracts the material state to the CS state, where Eqn. (13) yields $\phi_{ic} = \phi_c$ and Eqn. (25) yields $\beta = 0$, i.e. a stationary condition at the critical state.

The model was implemented in Plaxis as an user define constitutive model. A fully implicit one step backward-return algorithm was developed for the time integration of the constitutive equations.

4.2 Validation

While the plastic formulation is of standard design, the hyperelastic formulation is somewhat atypical and requires some sort of validation for the intended purpose.

To comply with this requirement, the natural period T of a number of symmetric triangular dams was computed numerically. Slope inclination and height were varied in the ranges $B = \{1.4:1, 1.6:1, 1.8:1\}$ and $H = \{50m, 75m, 100m, 125m, 150m\}$. The models were excited with a short base pulse and left free to oscillate. A fix set of material parameters was used, as follows: $e_{min} = 0.10$, $e_{max} = 0.40$, $c_s = 750$, $c_e = 2.17$, $m = 0.50$, and an unit weight $\gamma = 27 \text{ KN/m}^3 / (1 + e)$. Three void ratios $e = \{0.15, 0.20, 0.25\}$ were used. The product of five heights, three slopes and three void ratios yields 45 runs. The natural period was determined as the inverse of the dominant frequency of the output crest displacements. Fig. 3 shows the results, normalized by the prediction of Eqn. (6) for a shear wave velocity computed with Eqn. (10) and a pressure $p = \frac{2}{3}\gamma H$ equal to the weight of rockfill column above the baricenter of the dam.

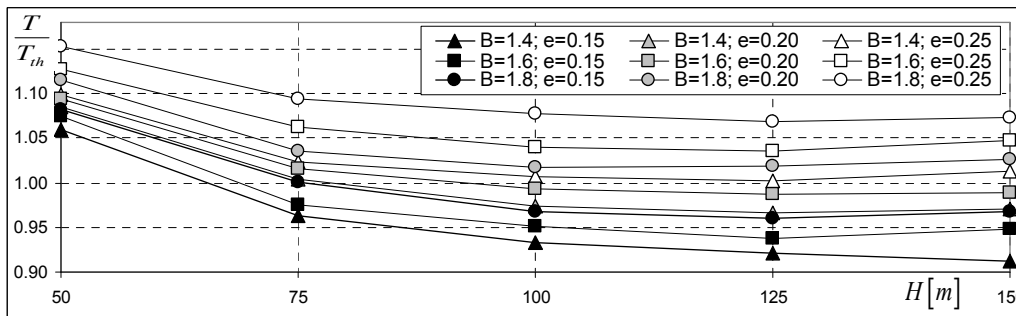


Fig. 3. Numerically computed natural periods T normalized by T_{th} given by Eqn (6).

5 Suggested design procedure

A procedure for the preliminary estimation of the earthquake-induced settlement of CFRDs is as follows: i) Compute the natural period of the dam using Eqns (7) (8) (10) and $p = \frac{2}{3}\gamma H$; ii) Compute the effective number of pulses N using Eqn. (9); iii) Build and load the model with a sine wave of amplitude $0.8PGA$, period T and duration $t = NT$; iv) Let the model oscillate freely for a time span $t = NT$; and v) Obtain the crest settlement at the end of the simulation. For simplicity, no recommendations are included here w.r.t. numerical issues as type and size of elements, boundary conditions, integration methods, or otherwise.

6 Case study

Los Caracoles dam is a CFRD located in San Juan, Argentina, in an area of high seismicity. The main dimensions of the dam are: $H = 140m$, $l_c = 620m$, $l_b = 130m$. Upstream slope is 1.5:1 and downstream slope is 1.7:1 with two berms. The design earthquake has a magnitude $M = 7.7$ and a $PGA = 1.02g$. Material parameters, computed or estimated with the information available at design stage (Bissio and Tejada, 2006), are shown in Table 2. G_{av} is the average shear modulus computed using Eqn. (10) with $p = \frac{2}{3}\gamma H$. The mesh and zone identification is shown in Fig. 4. It is worth noting that a simple mesh is used because the constitutive model accounts for all material nonlinearities that would otherwise require sub-division of the mesh and the definition of a large set of zones with different material properties.

Table 2. Material properties. Los Caracoles dam.

		e_{min}	e_{max}	c_s	c_e	m	ϕ_c	p_r	e	G_{av} [MPa]	v_s [m/s]
3B	alluvium / colluvium	0.10	0.45	650	2.17	0.5	41.3°	5.7	0.16	1060	670
3D	blasted greywacke	0.10	0.45	600	2.17	0.5	41.0°	2.5	0.20	890	625
3L	colluvium	0.10	0.40	650	2.17	0.5	36.5°	3.7	0.20	960	650
Riverbed	aged alluvium	0.12	0.46	700	2.17	0.5	37.1°	4.0	0.20	1040	675

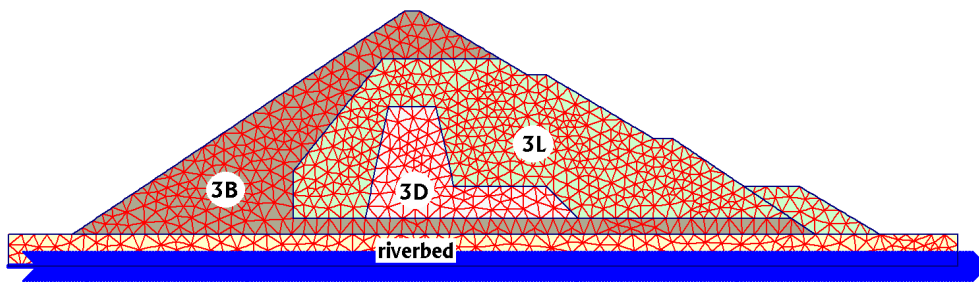


Fig. 4. Mesh and zonification, Los Caracoles Dam.

The natural period computed with Eqn. (8) is $T = 0.56s$. A sinusoidal acceleration of amplitude $0.8g$, period $T = 0.56s$ and duration $t = 7T$ was applied horizontally at the base of the model. The model was then allowed to oscillate freely for another $t = 7T$. The resulting settlement is $\delta = 2.38m$. This result can be compared with an analytical prediction of $\delta = 2.57m - 3.39m$ (Núñez, 2007) and a numerical estimation with an involved decoupled analysis of $\delta = 2.13m$ (Bissio and Tejada, 2006). One hour was needed to build and run the model and obtain the final results.

7 Conclusions

Design of CFRDs for earthquake loading is mainly based on experience and engineering judgement. Freeboard allowance for earthquake-induced settlements, however, must be verified at design stage. While methods used range from simple analytical tools to involved 3D models, simple numerical tools that account for dam zonification and irregular dam shapes can be used for convenience.

The numerical procedure presented is based on a simple constitutive model that includes pressure dependent elasticity in the pre-failure regime and hardening-softening isotropic plasticity combined with stress-dilatancy theory in the post-failure regime, and thus is applicable to geometries and materials where only monotonic plasticity is expected to occur, as is the case of CFRD dams.

The actual earthquake design record is replaced by a simple sinusoidal base acceleration having an equivalent effect on the dam. For simplicity, only CFRDs resting on hard rock are considered. The suggested procedure, however, can accommodate any foundation type.

A case study is presented where the procedure is applied to a CFRD 140 m high, located in Argentina and designed for a strong earthquake. The computed settlement compares well with an analytical estimation and with a decoupled numerical model of the same problem. The main advantage of the proposed procedure is that all material nonlinearities are accounted for by the constitutive equations, thus allowing for the usage of a simple mesh with no artificial sub-zonification.



8 Acknowledgements

E. Núñez shared his experience on earth dams with the author and provided comments to the procedure described in this paper. G. Weber co-authored several aspects of the implementation of the constitutive model used. J. Laiún co-worked in the numerical simulations. Their contributions is gratefully acknowledged.

9 References

- Bissio J., Tejada, C. 2006. Caracoles, análisis dinámico de la presa. Proc. IV Conf. CAP, Posadas (Argentina), 57-74.
- Bolton M. 1986. The strength and dilatancy of sands. *Geotechnique* **36**(1), 65-78.
- Bolton M. 1987. The strength and dilatancy of sands, Discussion. *Geotechnique* **37**(2), 219-226.
- Brinkgreve R. 2002. *Plaxis users manual*. Balkema, Rotterdam (The Neetherlands).
- Cooke J. 1984. Progress in rockfill dams. *ASCE JGE*, **110**(10), 1381-1414.
- Cooke J., Sherard J. 1987. Concrete-face rockfill dam: II. Design. *ASCE JGE*, **113**(10), 1113-1132.
- Cooke J. 1997. The concrete face rockfill dam. Proc. 17 USCOLD Lect., San Diego (USA), 117-132.
- De Beer E. 1965. Influence of the mean normal stress on the shearing resistance of sand. Proc. VI ICSMFE, Montreal (Canada), **1**, 165-169.
- Duncan J., Chang C. 1970. Non-linear analysis of stress and strain in soil. *ASCE JSMFD*, **96**(5), 1629-1653.
- Duncan J., Byrne P., Wong K., Mabry P. 1980. *Strength, stress-strain and bulk modulus parameters for finite element analyses of stresses and movements in soil masses*. Report UCB/GT/80-01, Univ. of California at Berkeley.
- Gazetas G., Dakoulas P. 1992. Seismic analysis and design of rockfill dams: State of the art. *Soil Dyn. Earthq. Eng.*, **11**(1), 27-61.
- Hardin B., Richart F. 1963. Elastic wave velocities in granular soils. *ASCE JSMFD*, **89**(1), 33-65.
- Kokusho T. 1980. Cyclic triaxial test of dynamic soil properties for wide strain range. *Soils and Foundations*, **20**(2), 45-60.
- Leps T. 1970. Review of Shearing Strength of Rockfill. *ASCE JSMFD*, **96**(4), 1159-1170.
- Makdisi F., Seed B. 1978. Simplified procedure for estimating dam and embankment earthquakes induced deformation. *ASCE JGE*, **104**(7), 849-867.
- Marsal R. 1967. Large scale testing of rockfill materials, *ASCE JSMFD*, **93**(2), 27-43.
- Matsuoka H., Nakai T. 1974. Stress-deformation and strength characteristics of soil under three different principal stresses. *Proc. Japan Soc. of Civil Eng.*, **232**, 59-70.
- Molenkamp F. 1988. A simple model for isotropic non-linear elasticity of frictional materials. *IJNAMG.*, **12**(5), 467-475.
- Newmark N. 1965. Effects of earthquakes on dams and embankments. *Geotechnique* **15**(2), 139-160.
- Núñez E. 2007. Behavior of coarse alluvium slopes subjected to earthquakes. Proc. XIII PCSMGE, Margarita (Venezuela), 862-867.
- Núñez E. 2007b. Uncertainties and approximations in geotechnics. Proc. XIII PCSMGE, Margarita (Venezuela), 26-39.
- Rowe P. 1962. The stress dilatancy relation for static equilibrium of an assembly of particles in contact. *Proc. Royal Soc. London*, 269, 500-527.
- Seed H. 1979. Considerations in the earthquake-resistant design of earth and rockfill dams. *Geotechnique* **29**(3), 215-283.
- Seed H., Wong R., Idriss I. Tokimatu K. 1984. *Moduli and damping factors for dynamic analyses of cohesionless soils*. Report UCB/EERC-84/14, Univ. of California at Berkeley.
- Sfriso A. 2007. A constitutive model for sands: Evaluation of predictive capability. Proc. XIII PCSMGE, Margarita (Venezuela), 242-247.
- Sherard J. Cooke J. 1987. Concrete-face rockfill dam: I. Assessment. *ASCE JGE*, **113**(10), 1096-1112.
- Uddin N., Gazetas G. 1995. Dynamic response of CFRD to strong seismic excitation. *ASCE JGE*, **121**(2), 185-197.
- Verdugo R., Ishihara K. 1996. The steady state of sandy soils. *Soils and Found.* **36**(2), 81-91.